Prediction of braid pattern on mandrels with constant non-circular cross-sections

J Hajrasouliha[1,a] , R Jafari Nedoushan[2] & M Sheikhzadeh[1]

[1] Department of Textile Engineering, [2] Department of Mechanical Engineering, Isfahan University of Technology,
Isfahan 84156-83111, Iran

In this study, a new useful mathematical model has been developed to predict the braid pattern for every point onto the mandrel surface with non-circular cross-sections. The Reza-Jalil-Mohammad (RJM) equation thus obtained has been proposed for the braid angle. The implementation and validation of this mathematical model has been discussed for a cylindrical mandrel. It is observed that using RJM equation, one can get the arrangement of strands in circular braiding machine for each mandrel with different cross-sections.

Keywords: Braid angle, Circular braiding machine, Mandrel, Non-circular cross-sections

1 Introduction

A braid is a complex structure or pattern formed by interlacing three or more strands of flexible materials, such as fibre, yarn and wire. Fundamentally, braid is a system of three or more strands intertwined in such a way that no two strands are twisted around one another[1].

The braid structures can be flat or tubular and have many applications due to good properties, such as high strength, low elongation, suitable formability, ease of recapping molds with various cross-sections, ease of modeling in finite element software for the prediction of mechanical properties of the created product, no restriction on the angle between the used strands in structures of braid, etc[2,3].

Circular braiding, a well-established textile process for forming tubular fabrics, has been extended to produce a range of structural shapes for composite applications in the fields including medicine, candles, civil engineering communities, transport and especially aerospace[4-7].

In 2D circular braiding, strands (reinforcement yarns) are wound on to spools or carriers mounted on a track plate around a central mandrel. Carriers are driven by horn gears and follow a serpentine path around the track plate[8]. Half of the strands move clockwise and form a braid angle of $(+\theta_b)$ with the mandrel axis, and the other half moves in a counter clockwise manner, forming a braid angle of $(-\theta_b)$

———————

[a]Corresponding author.
E-mail: j.hajrasouliha@tx.iut.ac.ir

with the mandrel axis. These two strand groups $(\pm\theta_b)$ are interlocked to form a biaxial fabric on the mandrel, as shown in Fig. 1(ref. 9).

Few technical works have been focused on the braiding process and the braid structure. The work done by Brunnschweiler[10,11] in the 1950s is still the most detailed research. Some authors have presented models for simple circular braiding, but they are not suitable for the mandrel with non-circular cross sections[5,12,13]. Michaeli and Rosenbaum[14] developed an algorithm for the control of a braiding machine. Although the control algorithm relates the machine speeds and mandrel shapes with braid angles to some extent, it does not provide a process model, covering all parameters for both the braiding process and the braid structure. Also, it cannot answer the fundamental question of why, under certain conditions, braiding over a mandrel with non-circular cross section is difficult or even impossible. Du et al.[15] considered mandrels of a circular section whose diameter varied along the length of the mandrel. They developed equations relating the positions and speeds of the mandrel, carriers, and strands at any given time to the braid angle of the fabric formed at that time. They used differential equations to describe the rate of growth of the fabric. They used a technique to numerically integrate the latter equations and also employed the former equations to calculate the set of braid angles along the length of the mandrel. Soebroto et al.[16] created an integrated design system for braided tubular composites. They developed design curves relating braiding parameters to braid geometry and

Fig. 1 — Schematic of a circular braiding machine[17]

experimentally verified them. The simulation of the circular braiding process as applied by the tool is still based on kinematic modeling only[16-24]. However, these studies have not presented a specific mathematical equation which could be applied in determination of braid angle for constant non-circular cross sections. Hence, the current study is aimed at presenting an applicable equation for the determination of braid angle in order to use this in stress analysis of braided composites in finite element software; an explicit and applicable equation for non-circular cross sections, is required. In other words, an equation is required to achieve the braid angle by giving geometric coordinates of cross-sections points.

As shown in Fig. 1 (circular braiding machine), the mandrel with a circular cross-section (supported by a holder) is located between the carriers and is concentric with the track plate. The mandrel moves with an axial velocity (*V)*. The strands are driven by spools or carriers with an angular velocity of $\pm \omega_c$.

For a mandrel having a circular cross-section with radius (*R*), the braid angle (θ_b) (Fig. 1), which is the most important parameter for getting physical and mechanical properties in braid structures, can be determined as follows:

$$\tan(\theta_b) = \frac{R\omega_c}{V} \qquad\qquad \dots (1)$$

It can be written as:

$$\tan(\theta_b) = \frac{2\pi R}{B_V} \qquad\qquad \dots (2)$$

where B_V is the braid feed, which is defined as the ratio of the axial velocity and the angular velocity of the braider (i.e. length of mandrel covered per revolution).

A geometric approach can be used to determine perpendicular spacing between strands (center-line spacing in Fig. 1), as shown below:

$$S_c = \frac{4\pi R}{N}\cos(\theta_b) \qquad\qquad \dots (3)$$

where *N* is the number of carriers in a circular braiding machine. The Eq. (3) can be used to determine the degree of the coverage of the mandrel, and it can also be used as the first approximation to anticipate strand locking[9].

It is clear that braid angle and perpendicular spacing between strands for a mandrel with constant circular cross-section (S_c) are invariable. But in many industries, especially in aerospace industry where composite structures are used in such different parts as fuselage, stringers, ribs, tail, wing skin, flaps, etc. 2-D braid structures can be used. In other words, by using a circular braiding machine, many of these can be braided and then through different methods of giving resin, especially RTM, resin could be injected to make the desired part. But the fundamental point is that in order to make different parts using circular braiding machine, many of these parts have a non-circular cross-section. Hence, changing the braid angle and the perpendicular spacing between strands in every point should be done in a simple and practical way. To put it more exactly, when a mandrel with a constant non-circular cross-section is used, braid angle and perpendicular spacing between strands (S_{nc}) are variable for every point on the mandrel surface. In the other words, the braid pattern

varies in every point on the mandrel surface and finding the braid pattern for these mandrels is an important and practical task.

In view of above, present study has been undertaken to develop new useful mathematical model to predict the braid angle and perpendicular spacing between strands in the braiding of a mandrel with constant non-circular cross-section. Finally, the implementation and validation of this mathematical model has been discussed for a cylindrical mandrel.

2 Materials and Methods

2.1 Model Assumptions
This mathematical model is based on the following basic assumptions:
(i) Geometry of mandrel cross-section is differentiable.
(ii) Yarn path from carrier to mandrel surface is continuous and differentiable.
(iii) Yarn path from the carrier to the fell point (the point on the mandrel surface wherein the braid pattern is formed) onto the mandrel surface (convergence zone) is straight and this straight line is tangent in the fell point.
(iv) As soon as the yarn touches the mandrel surface, it sticks to the mandrel surface.
(v) Braid pattern on the mandrel surface is differentiable.

The first assumption implies that the geometry of mandrel cross-section has no edges and dents on the mandrel surface. The second assumption shows that the yarn path has certain smoothness without any kinks. The third assumption implies that sufficient tension is applied on to the braiding yarns, and therefore they are tangent to the mandrel surface in the fell point. The fourth assumption implies that the yarn does not slip relative to the mandrel and the last assumption implies that the braid pattern is formed smoothly with no yarn kinks on the mandrel surface.

2.2 Braiding Process
Figure 2 shows a model of a circular braiding machine representing braiding a mandrel with constant non-circular cross-section, as shown by the differentiable equation $y_m = f(x_m)$. It is assumed that the yarns are straight, and hence have no interaction to avoid the complexity of figure. It is sufficient to describe the position of a carrier at a small time interval ($\Delta t \rightarrow 0$). In this case, it can also be assumed that the carriers rotate over the guide ring with radius R_g, instead of rotating on the track plate.
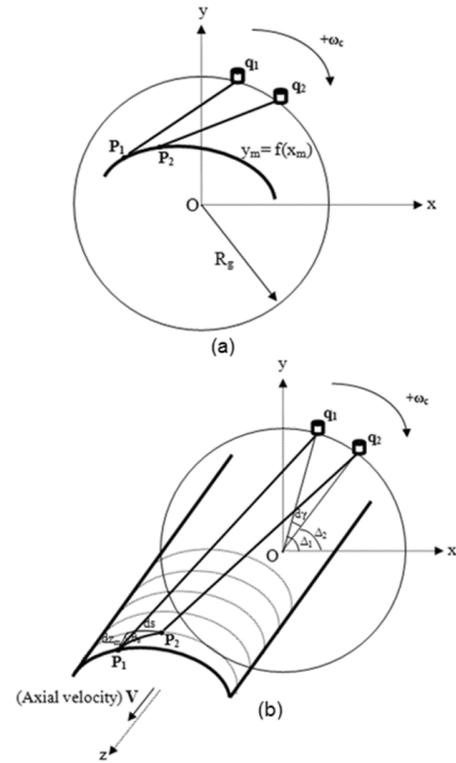
Fig. 2 — Schematic diagram of braiding process and parameters for a mandrel with an non circular cross sections $y_m = f(x_m)$ [(a) front view, and (b) top view]

As shown in Fig. 2, the carrier initially is in the position of q_1 on the guide ring and strand is in the position of P_1 on the mandrel surface; after Δt second, carrier is in the position of q_2 on the guide ring and strand is in the position of P_2 on the mandrel surface. Accordingly, a mandrel with the equation of cross-section $y_m = f(x_m)$ and axial velocity V is braiding.

2.3 Mathematical Relations
As discussed for model assumptions and braiding process, when the carrier rotates on the guide ring (quantity $d\gamma$), mandrel moves in z direction (quantity dz_m), and the strand lies on mandrel surface from P_1 to P_2 to form an almost straight line [Fig. 2(b)]. Accordingly, the braid angle for any point from the mandrel surface can be determined as follows:

$$\tan(\theta_b) = \frac{ds}{dz_m} \qquad \qquad \dots (4)$$

As shown in Fig. 2(b), the slight movement on the cross section of mandrel is ds, which has been created from the rotation of the carrier (quantity $d\gamma$) and the movement of the strand from P_1 to P_2. On the

other hand, from the definition of B_V, it can be concluded that:

$$dz_m = d\gamma \frac{B_V}{2\pi} \qquad \dots (5)$$

Following equation can be derived for braid angle, by substituting Eq. (5) in Eq. (4):

$$\tan(\theta_b) = \frac{ds}{d\gamma} \cdot \frac{2\pi}{B_V} \qquad \dots (6)$$

As shown in Fig. 2(b), $\frac{ds}{d\gamma}$ can be written as follows:

$$\Delta_1 = \Delta_2 + d\gamma \qquad \dots (7)$$

$$\frac{ds}{d\gamma} = k \frac{ds}{d\Delta} \qquad \dots (8)$$

where $k = \pm 1$.

The value of k depends on direction of carrier rotation (clockwise or counter-clockwise) and carrier position in quadrant. Figures 3(a) and (b) show k values for different rotation directions of carrier. Therefore, Eq. (6) can be rewritten as follows:

$$\tan(\theta_b) = k \frac{ds}{d\Delta} \cdot \frac{2\pi}{B_V} \qquad \dots (9)$$

According to the third assumption, the slope of tangent at any point of the mandrel surface $[f'(x_m)]$ is equal to the slope of yarn path from carrier to that point on the mandrel surface. Therefore, equation of yarn path from carrier to the point on mandrel surface (x_m, y_m) can be written as follows:

$$y_y = f'(x_m)x_y + b(x_y) \qquad \dots (10)$$

where $b(x_y)$ is the intercept of equation of yarn path.

In this study, the subscript y is indicative of yarn path from carrier to the mandrel surface, and the subscript m represents points on the mandrel surface.

As mentioned in the braiding process, it is assumed that in a circular braiding machine, carriers rotate over the guide ring with radius R_g; hence the movement path of the carriers is in the following circle:

$$X_c^2 + Y_c^2 = R_g^2 \qquad \dots (11)$$
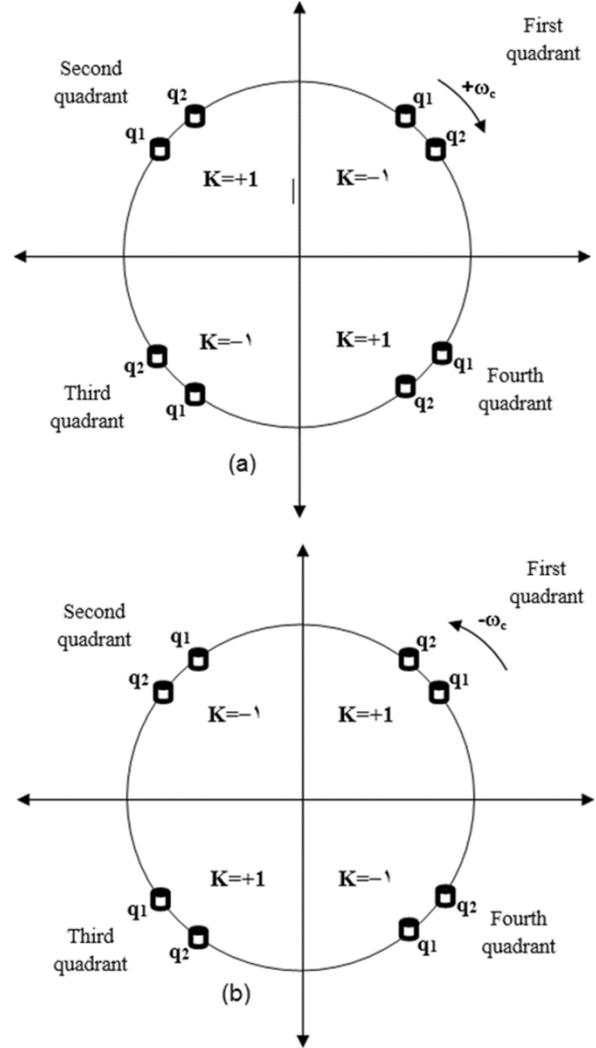
Fig. 3 — Value of k (a) clockwise, and (b) counter-clockwise

It should be noted that the subscript c is indicative of carrier. As shown in Fig. 2, at any moment, yarn path from carrier to point on the mandrel surface y_y intersects the movement path of carriers in the points q. With simultaneous solution of Eq. (10) and Eq. (11), coordinates of q can be calculated as:

$$\begin{cases} y_y = f'(x_m)x_y + b(x_y) \\ X_c^2 + Y_c^2 = R_g^2 \end{cases} \rightarrow$$

$$\begin{cases} Y_c = f'(x_m)X_c + y_m - f'(x_m)x_m \\ Y_c^2 = R_g^2 - X_c^2 \end{cases} \rightarrow \begin{bmatrix} X_{cq} \\ Y_{cq} \end{bmatrix} \qquad \dots (12)$$

For any point on mandrel surface (x_m, y_m), the corresponding point on movement path of carriers (X_{cq}, Y_{cq}) can be calculated. Delta angle (Δ) can be defined as follows [Fig. 2(b)]:

$$\Delta = \tan^{-1}(\frac{Y_{cq}}{X_{cq}}) \qquad \dots (13)$$

$$\frac{d\Delta}{dx_m} = \Delta' \qquad \dots (14)$$

On the other hand, the relationship between dx_m, dy_m and ds (Fig. 4) can be determined as follows:

$$ds^2 = dx_m^2 + dy_m^2 \qquad \dots (15)$$

$$ds^2 = dx_x^2 + [f'(x_m)dx_m]^2 \qquad \dots (16)$$

$$\frac{ds}{dx_m} = \sqrt{1 + [f'(x_m)]^2} \qquad \dots (17)$$

By considering Eqs (14) and (17), $\frac{ds}{d\Delta}$ can be written as follows:

$$\frac{ds}{d\Delta} = \frac{ds}{dx_m} \cdot \frac{dx_m}{d\Delta} = \frac{\sqrt{1 + [f'(x_m)]^2}}{\Delta'} \qquad \dots (18)$$

Finally, according to Eqs (9) and (18), braid angle in any point of mandrel surface can be written as follows:

$$\tan(\theta_b) = k \frac{\sqrt{1 + (f'(x_m))^2}}{\Delta'} \cdot \frac{2\pi}{B_V} \qquad \dots (19)$$

Using Eq. (19), braid angle in any point of a mandrel with the constant non- circular cross-section can be determined. Equation (19) obtained for the first time in this study, is named as the Reza-Jalil-Mohammad (RJM) equation.

Figure 5(a) shows part of the opened schematic from a mandrel with the circular cross-section. In a mandrel with the circular cross-section, perpendicular spacing between strands (s_c) is constant and can be calculated by Eq. (3). When a mandrel has a non-circular cross-section, perpendicular spacing between strands (s_{nc}) is different in any point [Fig. 5(b)], and it can be calculated by RJM equation, as follows:
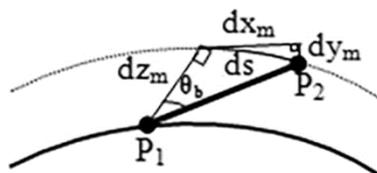
Fig. 4 — Geometry relationship between variations of x_m , y_m and ds

$$S_{nc} = \frac{2B_V}{N} \sin(\theta_b) \qquad \dots (20)$$

$$S_{nc} = \frac{2B_V}{N} \sin(\tan^{-1}(k \frac{\sqrt{1 + (f'(x_m))^2}}{\Delta'} \cdot \frac{2\pi}{B_V})) \qquad \dots (21)$$

As shown in Fig. 5(b), with increasing the braid angle in a mandrel with non- circular cross-section, perpendicular spacing between strands (s_{nc}) is increased and vice versa.

3 Results and Discussion

In order to verify the RJM equation, a mandrel with a constant circular cross-section was evaluated (Fig. 1). Equation of the mandrel can be written as follows:

$$y_m = \pm\sqrt{R^2 - x_m^2} \qquad \dots(22)$$

If the upper half of the circle is considered:

$$y'(m) = f'(x_m) = \frac{-x_m}{y_m} \qquad \dots(23)$$
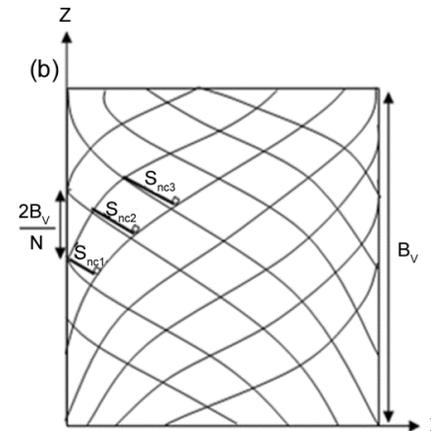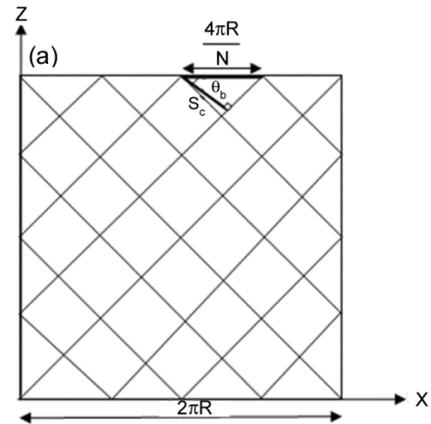
Fig. 5 — Part of the opened schematic from a braided mandrel with the (a) circular cross-section and (b) non-circular cross-section ($S_{nc1}<S_{nc2}<S_{nc3}$)

So, Eq. (12) for circle can be written as:

$$\begin{cases} Y_c = \dfrac{R^2 - x_m X_c}{y_m} \\ Y_c^2 + X_c^2 = R_g^2 \end{cases} \qquad \dots(24)$$

With simultaneous solution of Eq. (24), following equation is obtained:

$$R^2 X_c^2 - 2R^2 x_m X_c + R^4 - R_g^2 y_m^2 = 0 \qquad \dots(25)$$

As regards the upper half of the circle, the carrier rotation of direction clockwise, for a point on mandrel surface (x_m, y_m), X_{cq} and Δ can be calculated as follows:

$$X_{cq} = x_m + \frac{\sqrt{(R_g^2 - R^2)}}{R} y_m \qquad \dots(26)$$

$$\Delta = Arc\tan(\frac{Y_{cq}}{X_{cq}}) = Arc\tan(\frac{R^2 - x_m X_{cq}}{y_m X_{cq}}) \qquad \dots(27)$$

$$\frac{d\Delta}{dx_m} = \Delta' = \frac{(y_m X_{cq})(-X_{cq} - x_m X'_{cq}) - (R^2 - x_m X_{cq})(y'_m X_{cq} + y_m X'_{cq})}{(y_m X_{cq})^2 (1 + (\frac{R^2 - x_m X_{cq}}{y_m X_{cq}})^2)} \qquad \dots(28)$$

With substitution of Eqs (22), (23) and (26) in Eq. (28), Δ' can be written as follows:

$$\Delta' = \frac{-1}{y_m} \qquad \dots(29)$$

Finally, according to the RJM equation, braid angle for a mandrel with a constant circular cross-section is as follows:

$$\tan(\theta_b) = \frac{-\dfrac{R}{y_m}}{-\dfrac{1}{y_m}} \times \frac{2\pi}{B_V} = \frac{2\pi R}{B_V} = \frac{R\omega_c}{V} \qquad \dots(30)$$

Eq. (30) is the same as Eq. (1) or Eq. (2), as obtained by the RJM equation.

The aim of the current research was to achieve a simple, applicable and usable equation to determine the braid angle on all the mandrels with non-circular cross-sections (either axisymmetric or non-axisymmetric, either geometrically defined cross-sections or not geometrically defined cross-sections) and the constant length which has no dent or edge. This equation (RJM) is very useful and by solving this equation, the braid angle could be simply predicted in any locations. It could also be applied in common software for modelling and further analyzing.

4 Conclusion

A new mathematical model has been developed using circular braiding process which relates process variables and mathematical model to predict the braid pattern on a mandrel with constant non-circular cross-section. The RJM equation has been developed, for the first time, for determining the braid angle in any point of a mandrel with the constant non-circular cross-section. For validation purpose, a mandrel with a constant circular cross-section is evaluated by the presented mathematical model.

Using RJM equation, one can get the arrangement of strands in the circular braiding machine for each mandrel with a differentiable cross-section, such that it can be used in mechanical analyses by engineering software.

References
1 Hajrasouliha J, Sheikhzadeh M, Moezzi M & Babaeian Amini A, *J Ind Text*, (2015) 1.
2 Lei X, Seong J K, Cheng H O & Sung K H, *J Compos Mater,* 46 (2012) 2255.
3 Hajrasouliha J, Sheikhzadeh M & Ajeli S, *J Text Inst,* 105 (2014) 729.
4 Du G W & Popper P, *J Compos Mater*, 85 (1994) 316.
5 Ko F K, *Braiding: Engineered Materials Handbook* (ASM International, USA), 1987, 519.
6 Rosenbaum U, *Braiding: Analysis of Processing Fiber Reinforced Composites* (Verlag TUV Rheinland Publishers), 1991.
7 http://www.wirefirst.com/newsdetail.php?ID=2949 (accessed on 11 October 2016).
8 Potluri P, Rawal A, Rivaldi M & Porat I, *Composites Part A,* 34 (2003) 481.
9 Long A C, *Composites Part A,* 32 (2001) 941.
10 Brunnschweiler D, *J Text Inst,* 44 (1953) 666.
11 Brunnschweiler D, *J Text Inst,* 45 (1954) 55.
12 Zhang Q, Beale D & Broughton R M, *J Manuf Sci E,* 121 (1999) 345.
13 Zhang Q, Beale D & Broughton R M, *J Manuf Sci E,* 121 (1999) 351.
14 Michaeli W & Rosenbaum U, *Proceedings, 34th International SAMPE Symposium* (SAMPE, Covina, CA), 1989, 1834.
15 Du G W, Popper P & Chou T W, *J Material Sci*, 26 (1991) 3438.
16 Soebroto H B, Hager T, Pastore C & Ko F, *Proceedings, 35th International SAMPE Symposium* (SAMPE International, USA), 1990, 687.
17 Akkerman R & Rodriguez B, *Proceedings, ESAFORM-10* (American Institute of Physics, USA), 2007, 1074.
18 van Ravenhorst J H & Akkerman R, *Composites Part A,* 64 (2014) 147.
19 Rawal A, Potluri P & Steele C, *J Ind Text,* 35 (2005) 115.
20 Rawal A, Potluri P & Steele C, *J Ind Text*, 36 (2007) 221.
21 Alpyildiz T, *Text Res J,* 82 (2012) 443.
22 Lamers E, *Proceedings, SAMPE Benelux Meeting* (SAMPE International, USA), 2012.
23 Na W J, Ahn H C, Jeon S Y, Lee J S & Kang H M, *Compos Sci Technol,* 91 (2014) 30.
24 Ning F, Potluri P, Yu W & Hearl J, *Text Res J,* (2016) 1.